Bloch-wall phase transition in the spherical model

D A Garanin†

Institut für Theoretische Physik, Universität Hamburg, Jungiusstraße 9, D-20355 Hamburg, Germany

Abstract. The temperature-induced second-order phase transition from Bloch to linear (Ising-like) domain walls in uniaxial ferromagnets is investigated for the model of D-component classical spin vectors in the limit $D \rightarrow \infty$. This exactly solvable model is equivalent to the standard spherical model in the homogeneous case, but deviates from it and is free from unphysical behaviour in a general inhomogeneous situation. It is shown that the thermal fluctuations of the transverse magnetization in the wall (the Bloch-wall order parameter) result in the diminishing of the wall transition temperature T_B in comparison to its mean-field value, thus favouring the existence of linear walls. For finite values of T_B an additional anisotropy in the basis plane x, y is required; in purely uniaxial ferromagnets a domain wall behaves like a two-dimensional system with a continuous spin symmetry and does not order into the Bloch one.

1. Introduction

The spherical model proposed in 1952 by Berlin and Kac [1] (see also [2, 3]) has been used extensively up to now as the only exactly solvable model describing the phase transition in three-dimensional magnetic systems. In contrast to the mean-field approximation (MFA), the spherical model describes, in a simplified manner, the thermal fluctuations of spins, which can be taken into account exactly due to their Gaussian nature. The technique for the consideration of *inhomogeneous* systems described by the spherical model was developed by Barber and Fisher [4] for surface-induced inhomogeneity in layered magnetics and elaborated by Abraham and Robert [5] for the problem of phase separation (i.e. domain wall (DW) formation) in the spherical model. Later the inhomogeneous states of the bounded spherical model induced by antiperiodic [6] and twisted [7] boundary conditions were investigated.

The results obtained for inhomogeneous states of the spherical model possess some unexpected features. The phase transition temperature T_c of a four-dimensional ferromagnetic slab consisting of $N \gg 1$ layers turns out to be higher than that of the bulk in the case of *free-edge* boundary conditions [4]. The two-domain state induced by the magnetic field $\pm H$ in two half-spaces is characterized by the DW width diverging and the domain magnetization vanishing in the limit $H \rightarrow 0$, i.e. in contrast to the underlying Ising model the spherical model does not exhibit phase separation [5]. As was argued already in [4], such features are the result of the global spin constraint [1], which obviously becomes not so good in the inhomogeneous case.

† E-mail address: garanin@physnet.uni-hamburg.de

Another version of the spherical model—the model of isotropic D-component classical spin vectors in the limit $D \to \infty$—was proposed by Stanley [8, 9], who showed that in the homogeneous case this model is equivalent to the spherical model by Berlin and Kac [1]. The normalization condition for a spin on a lattice site i, $|m_i| = 1$, becomes, in the case where $D \to \infty$, very similar to the global spin constraint, which is the reason for the equivalence of the two models. However, since the spin normalization condition does not mix the spin variables on different lattice sites, the D-vector model by Stanley with $D \to \infty$ is more physically appealing than the original spherical model. Moreover, the two models become non-equivalent in a general inhomogeneous situation, where, as was shown by Knops [10], the $D = \infty$ model corresponds to some generalization of the spherical model using a local spin constraint. This idea was substantiated in the work by Costache *et al* [11], who calculated the Curie temperature $T_c(N)$ of a ferromagnetic film of $N \gg 1$ layers with free boundary conditions in four dimensions using a set of independent spin constraints in each layer. The numerically calculated values of $T_c(N)$ monotonically increase with N to the bulk value $T_c(\infty)$, which is physically expected and differs from the result of Barber and Fisher [4] for the standard spherical model.

The further advantages of the D-vector model are the possibilities of consideration of finite-D and anisotropic systems. The latter is important, in particular, for the calculation of finite-size corrections to T_c of ferromagnetic films mentioned above in the actual three-dimensional case. Since such a film with $N < \infty$ is a two-dimensional system, the T_c corrections are finite only in the presence of the stabilizing uniaxial anisotropy [12]. In spite of its advantages in comparison to the standard spherical model, the D-vector model with $D \gg 1$ was much less used than mentioned. As exceptions one can cite the works by Abe and Hikami [13, 14] and by Okabe and Masutani [15] dealing with the $1/D$ expansion for three-dimensional systems and the work by Okamoto [16] where the uniaxial spherical model with a transverse field was considered.

It should be noted that practically all the researchers dealing with the *isotropic D-vector* model used the designations N or n instead of the original D. Such a modification is, however, not justified in a general anisotropic case, where the number n of the relevant order parameter components determining the symmetry and thus the universality class of a system can be different from D. As an example one can consider the rather general '$n - D$ model' [17, 18] having the first $n \leqslant D$ components coupled by the exchange interaction with equal strength and the remaining $D - n$ components 'free'. Among realizations of the $n - D$ model are, in particular, the $x - y$ model ($D = 3$, $n = 2$) and the plane rotator one ($n = D = 2$) belonging to the same universality class determined by n but having different values of T_c depending on both n and D. Correspondingly, in a general case the $1/n$ expansion of the critical indices is not the same as the $1/D$ expansion of non-universal quantities.

The general qualitative result of [5], the absence of the phase separation in the spherical model (but not the disappearance of the domain magnetization!), can be explained by the fact that this model behaves in the bulk like the *isotropic D* = ∞ model [8, 17], which obviously exhibits no phase separation. For the D-vector model the separation of a specimen into domains with opposite magnetizations by domain walls of a finite width requires an easy-axis anisotropy, which makes the intermediate orientation of the magnetization in the wall energetically unfavourable in comparison to that in domains. Clearly, this actual situation cannot be treated either with the help of the spherical model in its standard formulation [1], or as well as with the improved version [11, 19], which is equivalent to the *isotropic D* = ∞ model in the general inhomogeneous case.

The problem arising here—the study of the influence of thermal fluctuations on the

domain wall structure—is not only important for comparing the properties of different versions of the spherical model. The physics of domain walls at elevated temperatures is itself a rather interesting and unexplored area, whereas since the seminal work by Landau and Lifshitz [20] the majority of researchers have addressed the zero-temperature statics and dynamics of DWs based on the assumption of the constant magnitude of the magnetization in the wall.

The first theoretical investigation of the temperature variation of the structure of domain walls is due to Bulaevskii and Ginzburg [21], who with the help of the phenomenological version of the MFA, using a macroscopic Landau free energy in the vicinity of T_c, predicted a phase transition from Bloch to linear DWs in uniaxial ferromagnets at some $T_B < T_c$. Qualitatively this phase transition can be explained by the fact that the spins in the centre of a Bloch wall, which are forced to lie perpendicular to the easy axis, experience a molecular field smaller than in domains and hence order at some temperature T_B less than T_c, which leads to linear (Ising-like) walls (LW) in the region $T_B < T < T_c$. For ferromagnets whose anisotropy energy is much smaller than the exchange interaction, the LW temperature region is narrow.

The transition from Bloch to linear walls at $T = 0$ depending on the anisotropy was investigated by van den Broek and Zijlstra [22] with numerical methods. It was found that LWs are realized if the ratio of the anisotropy energy to the exchange one exceeds $\frac{2}{3}$; the DW width δ is, in this case, comparable with the lattice spacing a_0. Later this transition was discovered by Sarker *et al* [23] in the framework of a formal soliton theory independently of Bulaevskii and Ginzburg. The problem was also addressed by Niez and Lajzerowicz [24, 25], where the factor $\frac{2}{3}$ mentioned above was calculated analytically.

The first indirect experimental evidence for the transition from Bloch to linear domain walls was obtained from the optical observations of the temperature dependence of the period of the domain structure in YFeO$_3$ just below T_c [26]. Lately the LWs were observed in the dynamical susceptibility experiments on the low-temperature ferromagnets GdCl$_3$ [27] and LiTbF$_4$ [28]. In [29, 30] the DW mobility was calculated in the whole temperature range, which exhibited a deep minimum at T_B. Such a minimum was observed recently in the dynamical susceptibility experiments on the high-temperature Ba and Sr hexaferrites [31, 32].

Recent experiments also provided evidence of strong fluctuational effects about the DW phase transition. The transition temperature T_B was substantially lower than its mean-field estimate, and the critical index β_B of the Bloch-wall order parameter (the transverse magnetization in the centre of the wall) was about 0.1 in contrast to the MFA value $\frac{1}{2}$. Such strong fluctuations are not actually surprising since a domain wall is a two-dimensional object. The analysis by Lawrie and Lowe [33] using renormalization-group arguments has led to the clear result that a domain wall in a *biaxial* ferromagnetic model having an additional anisotropy in the x, y plane (which is usually the effective one due to the magnetostatic field [20]) belongs to the universality class of the two-dimensional Ising model, and hence one can expect $\beta_B = \frac{1}{8}$. In contrast, in a purely uniaxial model without the dipole–dipole interaction, a domain wall behaves like a two-dimensional plane rotator model and can show only the Kosterlitz–Thouless phase transition without ordering to a Bloch wall.

The absence of the long-range order (i.e. the transverse magnetization component) in a domain wall in a purely uniaxial ferromagnet can be demonstrated with the help of the linear spin-wave theory. The thermal disordering of Bloch walls is due to the so-called Winter magnons [34], the excitations localized on the domain wall with the dispersion law $\varepsilon_q^2 \propto Aq^2(Aq^2 + K_\perp)$ (A is the inhomogeneous exchange constant, $K_\perp$ is the in-

plane anisotropy constant and q is a two-dimensional wavevector). The first factor in ε_q^2 corresponds to the free translational motion of the wall and the second describes the rotation of the magnetization in the centre of the wall in the x, y plane. It can be seen that the number of Winter magnons, which in the classical case is proportional to $\int d^2q/\varepsilon_q$, diverges logarithmically at small q, if $K_\perp$ tends to zero. Thus, in a purely uniaxial ferromagnetic model the linear walls cannot order to the Bloch ones at any non-zero temperature. For a small non-zero in-plane anisotropy $K_\perp$ the shift of T_B from its MFA value due to fluctuations should be essential.

The aim of this work is to find an exact solution for the domain wall magnetization profile in biaxial ferromagnets at non-zero temperatures and their transition temperature T_B in the framework of the spherical model in its D-vector version. Instead of modifying the approach of [4, 5] based on the calculation of the partition function with the steepest-descent method, we will use the diagram technique for classical spin systems [17, 35]. This diagram technique, which is a generalization of the 'Ising part' of the spin operator diagram technique of Vaks *et al* [36, 37], makes it possible to locate and sum up all the diagrams surviving in the limit $D \to \infty$ and can be reformulated for our present purposes for inhomogeneous situations.

The approximation obtained by summing up such diagrams (without going to the limit $D \to \infty$) is the so-called self-consistent Gaussian approximation (SCGA), which was first formulated by Horwitz and Callen [38] for the Ising model ($D = 1$). SCGA yields rather good results for the thermodynamic quantities of the Ising [39] and the classical Heisenberg ($D = 3$) [40] models on three-dimensional lattices in the whole temperature range and can be of importance for a possible improvement of the presently obtained results for the domain wall structure in the spherical limit with regard to systems with finite D. A detailed description of the classical spin diagram technique and SCGA can be also found in a recent publication [18].

The rest of the paper is organized as follows. In section 2 the diagram technique for classical spin systems and the construction of SCGA in the inhomogeneous case is described. In section 3 SCGA is simplified for $D \to \infty$, and a closed system of equations for magnetization and the spin–spin correlation function describing the domain wall in the spherical limit is derived. In section 4 the magnetization profile of a fluctuating domain wall is calculated and the dependence of the transition temperature T_B on the anisotropy parameters is analysed. In section 5 further problems of the DW statics and dynamics at elevated temperatures are discussed.

2. Classical spin diagram technique and SCGA

The appropriate classical D-vector Hamiltonian with biaxially anisotropic ferromagnetic exchange interaction can be written in the form

$$\mathcal{H} = -\tfrac{1}{2} \sum_{ij} J_{ij} \left(m_{zi} m_{zj} + \eta m_{yi} m_{yj} + \sum_{\alpha=3}^{D} \eta_\alpha m_{\alpha i} m_{\alpha j} \right) \tag{2.1}$$

where i, j are the lattice sites, m_i is the normalized D-component vector, $|m_i| = 1$, the dimensionless anisotropy factors satisfy $\eta_\alpha < \eta < 1$ and all η_α are, for simplicity, taken to be equal to each other. For $D = 3$ equation (2.1) reduces to the anisotropic classical Heisenberg model. In the chosen geometry the average magnetization in the bulk is directed parallel or antiparallel to the easy axis z, in the centre of a Bloch wall it takes on one of two possible orientations along the second easy axis y. All variables describing the magnetization profile

of a plane DW are functions of the coordinate x only. The temperature-normalized molecular field $\boldsymbol{\xi}_i$ acting on a spin on the site i from its neighbours is given by

$$\boldsymbol{\xi}_i = -\frac{\partial(\beta\mathcal{H})}{\partial\boldsymbol{m}_i} = \beta \sum_j J_{ij}\left(m_{zj}\boldsymbol{e}_z + \eta m_{yj}\boldsymbol{e}_y + \sum_{\alpha=3}^{D} \eta_\alpha m_{\alpha j}\boldsymbol{e}_\alpha\right) \qquad (2.2)$$

where $\beta \equiv 1/T$ and $\boldsymbol{e}$ are unit vectors in appropriate directions. The mean-field approximation consists in neglecting fluctuations of the molecular field $\boldsymbol{\xi}_i$; replacing $m_{zj} \Rightarrow \langle m_{zj}\rangle$, $m_{yj} \Rightarrow \langle m_{yj}\rangle$ and $m_{\alpha j} \Rightarrow 0$ in (2.2), one arrives at the inhomogeneous Curie–Weiss equation

$$\langle\boldsymbol{m}_i\rangle = B(\xi_i)\boldsymbol{\xi}_i/\xi_i \qquad (2.3)$$

where $B(\xi)$ is the Langevin function. For small anisotropy $(1 - \eta \ll 1)$ the magnetization varies slowly on the scale of the lattice spacing, and the continuous approximation can be applied to (2.3). In this case the zero-temperature results of Landau and Lifshitz [20] and the finite-temperature ones of Bulaevskii and Ginzburg [21] for the DW magnetization profile are recovered (see below).

Fluctuations of the molecular field (2.2) can be taken into account within the framework of a perturbative scheme based on the diagram technique for classical spin systems [17, 18, 35]. The perturbative expansion of the thermal average of any quantity $\mathcal{A}$ characterizing a classical spin system (e.g. $\mathcal{A} = m_i$) can be obtained by rewriting (2.1) as $\mathcal{H} = \mathcal{H}_0 + \mathcal{V}_{\text{int}}$, where $\mathcal{H}_0$ is the MFA Hamiltonian with the averaged molecular field determined by (2.3), and expanding the expression

$$\langle\mathcal{A}\rangle = \frac{1}{\mathcal{Z}} \int \prod_{j=1}^{N} \mathrm{d}\boldsymbol{m}_j \, \mathcal{A}\exp(-\beta\mathcal{H}) \qquad |\boldsymbol{m}_j| = 1 \qquad (2.4)$$

in powers of $\mathcal{V}_{\text{int}}$. The averages of various spin vector components $\alpha, \beta, \gamma, \ldots = 1, \ldots, D$ on various lattice sites $i, j, k, \ldots$ with the Hamiltonian $\mathcal{H}_0$ can be expressed through spin cumulants, $\Lambda_{\ldots}$ (see below), in the following way:

$$\langle m_{\alpha i}\rangle_0 = \Lambda_{\alpha i}$$
$$\langle m_{\alpha i}m_{\beta j}\rangle_0 = \Lambda_{\alpha\beta i}\delta_{ij} + \Lambda_{\alpha i}\Lambda_{\beta j} \qquad (2.5)$$
$$\langle m_{\alpha i}m_{\beta j}m_{\gamma k}\rangle_0 = \Lambda_{\alpha\beta\gamma i}\delta_{ijk} + \Lambda_{\alpha\beta i}\Lambda_{\gamma k}\delta_{ij} + \Lambda_{\beta\gamma j}\Lambda_{\alpha i}\delta_{jk} + \Lambda_{\gamma\alpha i}\Lambda_{\beta j}\delta_{ki} + \Lambda_{\alpha i}\Lambda_{\beta j}\Lambda_{\gamma k}$$

etc, where δ_{ij}, δ_{ijk} etc are the site Kronecker symbols equal to 1 for all site indices coinciding with each other and to zero in all other cases. For one-site averages $(i = j = k = \cdots)$ equation (2.5) reduces to the well known representation of moments through cumulants (semi-invariants), generalized for a multi-component case. In the graphical language (see, for example, figure 1) the decomposition (2.5) corresponds to all possible groupings of small circles (spin components) into oval blocks (cumulant averages). The circles coming from $\mathcal{V}_{\text{int}}$ (the 'inner' circles) are connected pairwise by the wavy interaction lines representing the quantity $\eta_{\alpha\beta}J_{ij}$. In diagram expressions the summation over the coordinates i and component indices α of inner circles is carried out. One should not take into account disconnected diagrams (i.e. those containing disconnected parts with no 'outer' circles belonging to $\mathcal{A}$ in (2.4)), since these diagrams are compensated for by the expansion of the partition function $\mathcal{Z}$ in the denominator of (2.4). Consideration of numerical factors shows that each diagram contains the factor $1/n_s$, where n_s is the number of the symmetry group elements of a diagram (see equations (2.9) and (2.10), the symmetry operations do not concern outer circles). In the homogeneous case it is more convenient for practical calculations to use the Fourier representation and calculate integrals over the Brillouin zone
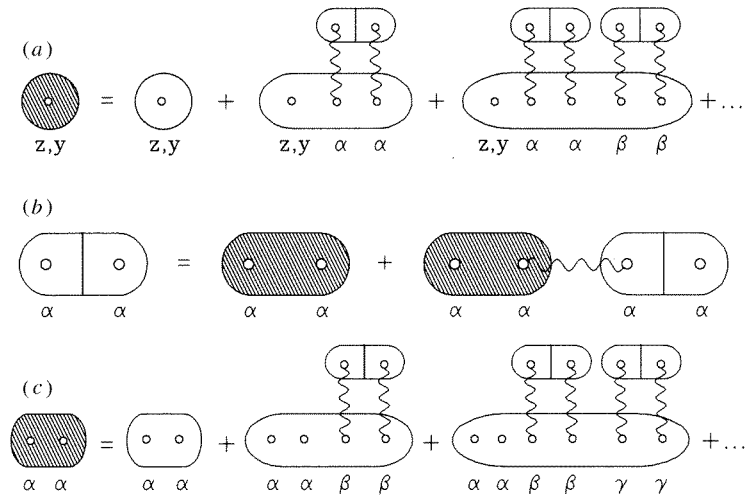
Figure 1. Self-consistent Gaussian approximation (SCGA) for classical spin systems. (*a*), (*c*) block summations for the renormalized magnetization and pair spin cumulant averages; (*b*): Dyson equation for the spin–spin correlation function.

rather than lattice sums. As the lattice sums are subject to the constraint that the coordinates of the circles belonging to the same block coincide with each other (due to the Kronecker symbols in (2.5)), in the Fourier representation the sum of wavevectors coming to or going out of any block along interaction lines is zero. The cumulant spin averages in (2.5) can be obtained by differentiating the generating function $\Lambda(\xi) = \ln \mathcal{Z}_0(\xi)$ over appropriate components of the dimensionless molecular field $\boldsymbol{\xi}$:

$$\Lambda_{\alpha_1 \alpha_2 .. \alpha_p}(\boldsymbol{\xi}) = \frac{\partial^p \Lambda(\xi)}{\partial \xi_{\alpha_1} \partial \xi_{\alpha_2} .. \partial \xi_{\alpha_p}} \tag{2.6}$$

where $\mathcal{Z}_0(\xi) = \text{constant} \times \xi^{-(D/2-1)} I_{D/2-1}(\xi)$ is the partition function of a D-component classical spin and $I_\nu(\xi)$ is the modified Bessel function. The two lowest-order cumulants which will be needed below can be written explicitly as

$$\Lambda_\alpha(\boldsymbol{\xi}) = B(\xi)\frac{\xi_\alpha}{\xi}$$

$$\Lambda_{\alpha\beta}(\boldsymbol{\xi}) = \frac{B(\xi)}{\xi}\left(\delta_{\alpha\beta} - \frac{\xi_\alpha \xi_\beta}{\xi^2}\right) + B'(\xi)\frac{\xi_\alpha \xi_\beta}{\xi^2} \tag{2.7}$$

where $\delta_{\alpha\beta}$ is the spin-component Kronecker symbol, $B(\xi) = \mathrm{d}\Lambda(\xi)/\mathrm{d}\xi$ is the Langevin function for D-component spins and $B'(\xi) \equiv \mathrm{d}B(\xi)/\mathrm{d}\xi$. The expressions for the three- and four-spin cumulants can be found in [35]. It should be stressed that the spin cumulants (2.7) appearing in the diagrams generated originally by the expansion of (2.4) in powers of $\mathcal{V}_{\text{int}}$ (the unrenormalized diagrams) simplify, since there are only a few non-zero components of the molecular field $\boldsymbol{\xi}$ (for a domain wall in the chosen geometry ξ_z and ξ_y). The complete form of spin cumulants (2.7) is needed, however, for the construction of SCGA allowing for the fluctuations of other components of the molecular field. For Ising systems the classical spin diagram technique coincides with the 'Ising part' of the standard SDT [36, 37] and can be used with Brillouin functions B_S of a general spin S. In the book [37] more technical details concerning the construction of SDT for Ising systems can be found, which play the same role in the present classical SDT.

The next step beyond MFA is the self-consistent Gaussian approximation taking into account *pair* correlations of the molecular field acting on a given spin from its neighbours, which implies the Gaussian statistics of the molecular field fluctuations (see figure 1). Since subsequently we are going to take the limit $D \to \infty$, only fluctuations of the molecular field components with $\alpha = 3, \dots, D$ should be taken into account, because their total contribution exceeds that of the fluctuations of z and y components by a factor of the order of D. The diagram sequence represented in figure 1 is equivalent to a closed system of nonlinear equations for the averaged magnetization $\langle \boldsymbol{m}_i \rangle$ and the correlation function $S_{ij}^{\alpha\alpha} \equiv \langle m_{\alpha i} m_{\alpha j} \rangle$ of the spin components with $\alpha = 3, \dots, D$. The diagrammatic equation in figure 1(*a*) is the generalization of the Curie–Weiss equation (2.3) for the magnetization (the angle brackets are dropped):

$$\boldsymbol{m}_i = \partial \tilde{\Lambda}(\boldsymbol{\xi}_i, l_{\alpha i}) / \partial \boldsymbol{\xi}_i = \tilde{\Lambda}_z(\boldsymbol{\xi}_i, l_{\alpha i}) \boldsymbol{e}_z + \tilde{\Lambda}_y(\boldsymbol{\xi}_i, l_{\alpha i}) \boldsymbol{e}_y \tag{2.8}$$

where the (averaged) molecular field $\boldsymbol{\xi}_i$ is given by the expression (2.2) without the last term and $l_{\alpha i}$ is related to the dispersion of the molecular field fluctuations on the site i:

$$l_{\alpha i} \equiv \frac{1}{2!} \langle \xi_{\alpha i} \xi_{\alpha i} \rangle = \frac{1}{2!} \eta_\alpha^2 \beta^2 \sum_{jj'} J_{ij} J_{ij'} S_{jj'}^{\alpha\alpha} . \tag{2.9}$$

The spin cumulant averages $\tilde{\Lambda}_{\dots}$ on a site i (see figures 1(*a*) and (*c*)) renormalized by Gaussian fluctuations of the molecular field are given by

$$\tilde{\Lambda}_{\dots} = \Lambda_{\dots} + \sum_{\alpha=3}^{D} \Lambda_{\dots\alpha\alpha} l_\alpha + \sum_{\alpha,\beta=3}^{D} \left(1 - \delta_{\alpha\beta} + \frac{1}{2!} \delta_{\alpha\beta} \right) \Lambda_{\dots\alpha\alpha\beta\beta} l_\alpha l_\beta + \cdots \tag{2.10}$$

where taking into account only the first term corresponds to MFA. These series, describing the influence of pair-correlated fluctuations of different components of the molecular field, can be rewritten as

$$\tilde{\Lambda}_{\dots} = \prod_{\alpha=3}^{D} \sum_{n_\alpha=0}^{\infty} \frac{1}{n_\alpha!} \left(l_{\alpha i} \frac{\partial^2}{\partial \xi_\alpha^2} \right)^{n_\alpha} \Lambda_{\dots}(\boldsymbol{\xi}_i) = \exp \left[\sum_{\alpha=3}^{D} l_{\alpha i} \frac{\partial^2}{\partial \xi_\alpha^2} \right] \Lambda_{\dots}(\boldsymbol{\xi}_i) . \tag{2.11}$$

Such exponential differential operators were considered by Horwitz and Callen [38] for the Ising model. Generalization of their results for the multi-component case yields a closed formula

$$\tilde{\Lambda}_{\dots} = \frac{1}{\pi^{(D-2)/2}} \int \mathrm{d}^{D-2} r \, \mathrm{e}^{-r^2} \Lambda_{\dots}(\boldsymbol{\zeta}_i) \tag{2.12}$$

where $\boldsymbol{\zeta}_i$ is the spread molecular field given by

$$\boldsymbol{\zeta}_i \equiv \boldsymbol{\xi}_i + 2 \sum_{\alpha=3}^{D} l_{\alpha i}^{1/2} r_\alpha \boldsymbol{e}_\alpha \tag{2.13}$$

and the integration in (2.12) is performed with respect to the $(D-2)$-component vector variable $\boldsymbol{r} \equiv \{r_\alpha\}$.

The Dyson equation for the spin–spin correlation function $S_{jj'}^{\alpha\alpha}$ entering (2.9) is represented in figure 1(*b*) and has the analytical form

$$S_{jj'}^{\alpha\alpha} = \tilde{\Lambda}_{\alpha\alpha j} \delta_{jj'} + \tilde{\Lambda}_{\alpha\alpha j} \eta_\alpha \beta \sum_r J_{jr} S_{rj'}^{\alpha\alpha} . \tag{2.14}$$

Applying this equation twice, one can simplify the expression for the quantity $l_{\alpha i}$ to

$$l_{\alpha i} = \frac{1}{2\tilde{\Lambda}_{\alpha\alpha i}} \left(\frac{S_{ii}^{\alpha\alpha}}{\tilde{\Lambda}_{\alpha\alpha i}} - 1 \right) . \tag{2.15}$$

The system of SCGA equations for a domain wall in a biaxial ferromagnet stated above simplifies for a small anisotropy $(1 - \eta \ll 1)$ and in the limit $D \to \infty$, which will be pursued in the next section. For $\eta_\alpha = 0$ the molecular field fluctuations measured by the quantity $l_{\alpha i}$ vanish according to (2.14) and (2.15), and the magnetization equation (2.8) reduces to the MFA result (2.3).

3. The spherical limit

In the spherical limit $D \to \infty$ the Langevin function $B(\xi)$ (see equations (2.3) and (2.7)) simplifies to

$$B(\xi) \cong \frac{x}{1 + \sqrt{1 + x^2}} \tag{3.1}$$

where the scaled variable x (which should not be confused with the coordinate x appearing below) is given by $x \equiv 2\xi/D$. Correspondingly, the spin cumulant averages (2.6) considered as functions of x can be estimated as

$$\Lambda_{\alpha_1 \alpha_2 \cdots \alpha_k} \propto D^{1-k} . \tag{3.2}$$

With the help of this estimate it can be shown that in the limit $D \to \infty$ SCGA becomes exact, since all other more complicated diagrams die out, at least as $1/D$ [35]. Indeed, a unification of two oval blocks into a larger one, which leads to a more complicated diagram (e.g. $\Lambda_{\alpha\alpha} \cdot \Lambda_{\beta\beta} \Rightarrow \Lambda_{\alpha\alpha\beta\beta}$ in figure 1), leads to the appearance of an additional factor $1/D$, since

$$\Lambda_{\alpha_1 \alpha_2 \cdots \alpha_{m+n}} \propto \Lambda_{\alpha_1 \alpha_2 \cdots \alpha_m} \cdot \Lambda_{\alpha_{m+1} \cdots \alpha_{m+n}}/D . \tag{3.3}$$

In [35] some such higher-order diagrams were considered in the framework of the $1/D$ expansion for low-dimensional classical ferro- and antiferromagnets.

For the consideration of the limit $D \to \infty$ it is convenient to introduce the well behaved dimensionless temperature variable $\theta \equiv T/T_c^{MFA}$, where $T_c^{MFA} = J_0/D$ and J_0 is the zero component of the exchange interaction, as well as the further D-independent variables:

$$G_i \equiv (D/\theta)\tilde{\Lambda}_{\alpha\alpha i} \qquad \tilde{l}_i \equiv l_{\alpha i}/D \qquad s_{ii'} \equiv DS_{ii'}^{\alpha\alpha} . \tag{3.4}$$

Expression (2.15) can now be rewritten as

$$\tilde{l}_i = \frac{1}{2\theta G_i}\left(\frac{s_{ii}}{\theta G_i} - 1\right) \tag{3.5}$$

and the expression for the square of the spread value of the argument x in (2.12) reads

$$x_i^2 \equiv \left(\frac{2\zeta_i}{D}\right)^2 = \left(\frac{2}{\theta}\sum_j \lambda_{ij}m_{zj}\right)^2 + \left(\frac{2\eta}{\theta}\sum_j \lambda_{ij}m_{yj}\right)^2 + \frac{16\tilde{l}_i}{D}\sum_{\alpha=3}^D r_\alpha^2 \tag{3.6}$$

where $\lambda_{ij} \equiv J_{ij}/J_0$. It can be seen that the contributions of the fluctuations of the α-components of the molecular field to (3.6) (each of them is small as $1/D$) are essential due to their large number. Now the Gaussian integrals (2.12) can be easily calculated (for $D \gg 1$) by applying the identity

$$\frac{1}{\pi^{1/2}}\int_{-\infty}^{\infty} dx\, e^{-x^2} f(ax^2) \cong f(a/2) \qquad a \ll 1 \tag{3.7}$$

successively $D - 2$ times. Thus, the integration leads simply to the replacement $r_\alpha^2 \Rightarrow \frac{1}{2}$ in (3.6). Now for the quantity G_i (equation (3.4)) with the use of the second equation of of (2.7) and the asymptotic expression (3.1) one gets

$$G_i = \frac{2}{\theta} \frac{1}{1 + \sqrt{1 + x_i^2}}. \tag{3.8}$$

The magnetization equation (2.8) can be simplified by using the first of equation of (2.7) and (3.1) to

$$m_{zi} = G_i \sum_j \lambda_{ij} m_{zj} \qquad m_{yi} = \eta G_i \sum_j \lambda_{ij} m_{yj}. \tag{3.9}$$

Finally, determining x_i^2 from (3.8) as a function of G_i, equating it to (3.6) with $r_\alpha^2 = \frac{1}{2}$ and using (3.5) and (3.9), one arrives at the equation

$$s_{ii} + m_i^2 = 1 \tag{3.10}$$

which is nothing but the kinematic identity $m_i^2 = 1$ in the limit $D \to \infty$. The normalized correlation function $s_{ii'}$ determined by (3.4) satisfies the following linear equation from (2.14),

$$s_{ii'} = \theta G_i \delta_{ii'} + \eta_\alpha G_i \sum_j \lambda_{ij} s_{ji'} \tag{3.11}$$

with the variable coefficient G_i. Equations (3.9)–(3.11) constitute the closed system of equations, which can be applied to the calculation of the domain wall magnetization profile in the spherical limit.

In the homogeneous case (or in one of the domains) $m_y = 0$ and m_z and G are constants. In this case equation (3.11) can be easily solved with the help of the Fourier transformation, which results in

$$s_{ii} = v_0 \int \frac{\mathrm{d}q}{(2\pi)^3} s_q = \theta G P(\eta_\alpha G) \qquad P(X) \equiv v_0 \int \frac{\mathrm{d}q}{(2\pi)^3} \frac{1}{1 - X\lambda_q} \tag{3.12}$$

where v_0 is the unit cell volume and $\lambda_q \equiv J_q/J_0$. In the long-wavelength limit $\lambda_q \cong 1 - \alpha q^2$, where $\alpha \sim a_0^2$ and a_0 is the lattice spacing. The lattice integral $P(X)$ has the following properties:

$$P(X) \cong \begin{cases} 1 + X^2/z & X \ll 1 \\ W - c_0 (1 - X)^{1/2} & 1 - X \ll 1 \end{cases} \tag{3.13}$$

where z coincides with the number of nearest neighbours NN for the NN interactions and W (the Watson integral) and $c_0 = v_0/(4\pi\alpha^{3/2})$ are lattice-dependent constants. For a simple cubic (SC) lattice $v_0 = a_0^3$ and $\alpha = a_0^2/6$, hence $c_0 = (2/\pi)(3/2)^{3/2}$. Since the sum in the right-hand part of the first equation of (3.9) equals m_z, this equation is satisfied only if $m_z = 0$ (above T_c) or $G = 1$ (below T_c). In these cases from equation (3.10) one gets the temperature-dependent magnetization $m \equiv m_z$:

$$m = (1 - \theta/\theta_c)^{1/2} \qquad \theta \leqslant \theta_c \equiv 1/P(\eta_\alpha). \tag{3.14}$$

It can be seen that in the fully isotropic case ($\eta = \eta_\alpha = 1$) the value of the phase transition temperature in the bulk $\theta_c = 1/P(\eta_\alpha)$ reduces to the well known result $\theta_c = 1/W$ [1].

The width of a Bloch wall δ_B in a uniaxial ferromagnet is determined by the balance between the anisotropy and inhomogeneous exchange energies. For small anisotropy $(1 - \eta \ll 1)$ the condition $\delta_B \gg a_0$ is fulfilled. In this case the change of the domain

wall magnetization at a distance of a_0 is small, and for systems with the nearest-neighbour interactions one can rewrite the lattice sum in (3.9) about some point $r \equiv r_i$ as

$$\sum_j \lambda_{ij} m_j \cong m(r) + \alpha \Delta m(r) \tag{3.15}$$

where the second term with the Laplace operator Δ is small in comparison to the first one. The quantity G_i in (3.9) determined by (3.4) is in the small-anisotropy case also a continuous function of the coordinate with the scale δ. Moreover, as can be seen from (3.9) and (3.15), the deviation of G from its bulk value 1 is small, i.e.

$$G(r) = 1 + G_1(r) \qquad G_1 \ll 1. \tag{3.16}$$

Now one can rewrite the equations (3.9) in terms of the normalized magnetization $n \equiv m/m_e$, where m_e is the equilibrium bulk magnetization given by (3.14). The result in the chosen geometry is of the form

$$\alpha n_z''(x) = -G_1(x) n_z(x)$$
$$\alpha n_y''(x) = -G_1(x) n_y(x) + (1 - \eta) n_y(x). \tag{3.17}$$

The kinematic equation (3.10) can be represented in terms of n as

$$\epsilon(1 - n^2) = \theta_c s_{ii}/\theta - 1 \qquad \epsilon \equiv \theta_c/\theta - 1. \tag{3.18}$$

Unlike the magnetization equation (3.9), the equation for the correlation function (3.11) cannot, in general, be written in a continuous form of the type (3.17). In the general case we are going to consider, where η_α is not necessarily close to 1, the correlation length of the α spin components below θ_c,

$$\xi_{c\alpha} = \sqrt{\alpha \eta_\alpha/(1 - \eta_\alpha)} \tag{3.19}$$

(not to be confused with components of the normalized molecular field ξ), which can be determined from s_q in (3.12), can be comparable with the lattice spacing a_0. Moreover, even in the case $1 - \eta_\alpha \ll 1$ the continuous approximation for $s_{ii'}$ does not yield the correct bulk result (3.12) which is formed by integration over the whole Brillouin zone and not only over the long-wavelength region $q \ll 1$. But it can, nevertheless, be applied for the calculation of the wall properties, as we shall see below.

4. Domain wall magnetization profile

Before proceeding to the solution of equations (3.17), (3.18) and (3.11) in the general situation, let us first consider the case $\eta_\alpha = 0$, where the spin fluctuations play no role and the situation is described exactly by MFA. Here the solution of (3.11) yields $s_{ii} = \theta G_i$, and with the help of (3.18) one gets $G_1(x) = \epsilon[1 - n^2(x)]$. Adopting it in (3.17) and solving the resulting equations, one arrives at the magnetization profile [21, 23]

$$n_z = \pm \tanh(x/\delta) \qquad n_y = \pm \rho/\cosh(x/\delta) \tag{4.1}$$

where

$$\rho = \begin{cases} \sqrt{1 - \tau} & \tau \equiv 2(1 - \eta)/\epsilon \leqslant 1 \\ 0 & \tau \geqslant 1 \end{cases} \qquad \delta = \begin{cases} \delta_B = \sqrt{\alpha/(1 - \eta)} & \tau \leqslant 1 \\ \delta_L = \sqrt{2\alpha/\epsilon} = \delta_B \tau^{1/2} & \tau \geqslant 1. \end{cases} \tag{4.2}$$

It can be seen that the crossover from the Bloch ($\rho = 1$) to the linear ($\rho = 0$) wall proceeds with increasing temperature through the elliptic one having $n_z^2 + n_y^2/\rho^2 = 1$ with $0 < \rho < 1$,

and the transverse component of the magnetization in the wall, n_y, disappears through a second-order phase transition. The temperature of the DW phase transition can be written in three forms:

$$\tau_B = 1 \qquad \epsilon_B = 2(1 - \eta) \ll 1 \qquad \theta_B = 1/(1 + \epsilon_B) \cong 1 - \epsilon_B \qquad (4.3)$$

the quantity τ playing the same role for a DW as the 'absolute' temperature θ for the bulk (cf equation (3.14)). The temperature-dependent factor ρ in (4.1) can be interpreted as the DW order parameter m_B [31, 32]. Whereas the Bloch-wall width δ_B is temperature-independent, the width of the linear wall δ_L is determined by the balance of the homogeneous and inhomogeneous exchange energies and is diverging at θ_c. Considering the first of equations (4.1) for $x \gg \delta_L$, one can identify

$$1 - \tanh(x/\delta_L) \cong \exp(-x/\xi_{cz}) \Longrightarrow \delta_L = 2\xi_{cz} \qquad (4.4)$$

where ξ_{cz} is the correlation length of the z spin components. One should also note the analogy between the Bloch-wall width δ_B (4.2) and the transverse correlation length $\xi_{c\alpha}$ (3.19), which coincide for a purely uniaxial ($\eta_\alpha = \eta$) model with small anisotropy. The function G_1 entering the equations (3.17) can be written as

$$G_1(x) = \frac{\epsilon(1 - \rho^2)}{\cosh^2(x/\delta)} = \frac{2\alpha}{\delta^2} \frac{1}{\cosh^2(x/\delta)}. \qquad (4.5)$$

Since $\alpha \sim a_0^2$, in the small-anisotropy case $G_1 \sim (a_0/\delta)^2 \ll 1$ in the whole temperature interval.

Now we proceed to the solution of the magnetic interface problem described by the equations (3.17), (3.18) and (3.11) in the general case $\eta_\alpha \neq 0$. The solution of the Dyson equation for the correlation function (3.11) depends on the relation between the correlation length $\xi_{c\alpha}$ (3.19) and the other length scales, a_0 and δ. If $\xi_{c\alpha} \gg a_0$, which is satisfied for $1 - \eta_\alpha \ll 1$, the continuous approximation to equation (3.11) can be applied. If $\xi_{c\alpha} \ll \delta$ (i.e. $1 - \eta_\alpha \gg 1 - \eta$, see (4.2)), the correlation function s_{ij} can be easily calculated *locally* with respect to the slowly changing magnetization profile (or, more exactly, the profile of G) in the wall. For uniaxial ferromagnets with a small anisotropy ($1 - \eta \ll 1$) considered throughout this paper these limiting cases overlap in the region $1 - \eta \ll 1 - \eta_\alpha \ll 1$. Let us consider first the case $\xi_{c\alpha} \ll \delta$. Here one can make a replacement $G_i \Rightarrow G_{i'}$ in (3.11), after which this equation can be solved as in the homogeneous case. With the use of (3.12) and (3.16) one gets

$$s_{ii} \cong \theta G_i P(\eta_\alpha G_i) \cong \theta P(\eta_\alpha)[1 + I(\eta_\alpha)G_1(x)] \qquad (4.6)$$

where

$$I(\eta_\alpha) = 1 + \frac{\eta_\alpha P'(\eta_\alpha)}{P(\eta_\alpha)} \cong \begin{cases} 1 + 2\eta_\alpha^2/z & \eta_\alpha \ll 1 \\ \dfrac{c_0}{2P(\eta_\alpha)} \dfrac{1}{\sqrt{1 - \eta_\alpha}} & 1 - \eta_\alpha \ll 1 \end{cases} \qquad (4.7)$$

and c_0 is determined by (3.13). Now with the use of (4.6) and (3.18) one can express G_1 through the magnetization profile $n(x)$:

$$G_1(x) = \epsilon[1 - n^2(x)]I^{-1}(\eta_\alpha). \qquad (4.8)$$

This expression differs only by a constant from that used in the beginning of this section in the MFA limit $\eta_\alpha = 0$. Solving now the magnetization equations (3.17) as above, one gets the same DW magnetization profile (4.1), where the parameters ρ and δ are given by (4.2)

with the renormalized DW temperature: $\tau \Rightarrow \tilde{\tau} \equiv \tau I(\eta_\alpha)$. The critical values of the three temperature variables (cf equation (4.3)) now read

$$\tau_B = I^{-1}(\eta_\alpha) < 1 \qquad \epsilon_B = 2(1-\eta)I(\eta_\alpha) \qquad \theta_B = \theta_c/(1+\epsilon_B) \qquad (4.9)$$

where θ_c is given by (3.14). One can see from (4.9) and (4.7) that for $1 - \eta_\alpha \ll 1$ the effective transition temperature τ_B becomes small. On the other hand, due to the validity condition $1 - \eta_\alpha \gg 1 - \eta$ the absolute temperature θ_B of the DW phase transition remains in the limiting case under consideration close to θ_c ($\epsilon_B \ll 1$). It can be seen that in this case the domain wall does not demonstrate any two-dimensional behaviour, and its phase transition at $\theta_B < \theta_c$ can still be described qualitatively by the effective diminishing of the ordering interaction for the wall spins forced perpendicularly to the easy axis z, as was said in the introduction. The effect in the case where $1 - \eta_\alpha \ll 1$ is much larger than according to the MFA estimates because of the divergence of the function $I(\eta_\alpha)$ (equation (4.7)). Accordingly, the width of the linear wall can considerably exceed its mean-field value (4.2):

$$\delta_L = \sqrt{\frac{2\alpha}{\epsilon}} I^{1/2}(\eta_\alpha) \cong \sqrt{\frac{\alpha c_0}{\epsilon P(\eta_\alpha)}} \frac{1}{(1-\eta_\alpha)^{1/4}} \qquad (4.10)$$

in the case where $1 - \eta_\alpha \ll 1$. Since δ_L is related to the longitudinal correlation length (see equation (4.4)), this result shows a non-trivial influence of fluctuations of transverse spin components on the longitudinal spin correlations in the anisotropic spherical model. One can also check that the function $G_1(x)$ (equation (4.8)) is still given by the expression (4.5) with the changed value of the DW width δ.

In the other limiting case, $\xi_{c\alpha} \gg a_0$, a continuous approximation of the type (3.15) can be applied to the Dyson equation (3.11). Making the Fourier transformation with respect to the coordinates y and z and using the conditions $1 - \eta_\alpha \ll 1$ and (3.16) one arrives at the differential equation for the correlation function

$$\alpha s''(x) - [1 - \eta_\alpha + \alpha q^2 - G_1(x)]s(x) = -\theta \delta(x - x') \qquad (4.11)$$

where $q^2 \equiv q_y^2 + q_z^2$ and the 'mute' argument x' of s was dropped. This equation should be solved to yield s with $x = x'$ as a function or functional of G_1, and s_{ii} (cf equation (4.6)) should be obtained by the integration of s over q_y and q_z. Then, as above, G_1 should be found from (3.18) and used in the magnetization equations (3.17). All this seems to be too complicated since equation (4.11) cannot be solved analytically for the arbitrary function $G_1(x)$. But the expected result that the DW transition temperature θ_B turns to zero in the purely uniaxial case $\eta_\alpha = \eta$ signals that there should be an exact solution to the problem. We can try to find it assuming that $G_1(x)$ has the same functional form as above, equation (4.5), with some renormalized value of the DW width δ as a parameter. Then using a new variable $u \equiv \tanh(x/\delta)$, equation (4.11) can be rewritten as

$$\frac{d}{du}(1 - u^2)\frac{ds}{du} + \left(2 - \frac{\mu^2}{1 - u^2}\right)s(u) = -\frac{\delta\theta}{\alpha}\delta(u - u') \qquad \mu^2 \equiv \frac{\delta^2}{\alpha}(1 - \eta_\alpha + \alpha q^2) \qquad (4.12)$$

and solved in terms of the adjoined Legendre functions

$$P_1^{\pm\mu}(u) = \frac{u \pm \mu}{\Gamma(2 \pm \mu)}\left(\frac{1+u}{1-u}\right)^{\pm\mu/2} \qquad (4.13)$$

which leads to

$$s(x, x', q) = \frac{\theta\delta}{2\alpha\mu}\exp\left(-\frac{\mu}{\delta}|x - x'|\right)\left[1 + \frac{1 - \tanh(x/\delta)\tanh(x'/\delta)}{\mu^2 - 1}\left(1 + \mu\tanh\frac{|x - x'|}{\delta}\right)\right]. \qquad (4.14)$$

This (not translationally invariant) expression can be reduced in the case $x = x'$ with the help of (4.5) to the form

$$s(x, x, q) = \frac{\theta}{2\alpha^{1/2}\sqrt{1 - \eta_\alpha + \alpha q^2}} \left[1 + \frac{G_1(x)}{2[1 - \eta_\alpha - (1 - \eta)/\tilde{\delta}^2 + \alpha q^2]} \right] \tag{4.15}$$

where $\tilde{\delta} \equiv \delta/\delta_B$ (see equation (4.2)). Since the structure of this expression is analogous to that of (4.6), it is now clear that the choice of G_1 in the form (4.5) was right. Integrating (4.15) over the two-dimensional wavevector q to get s_{ii} and proceeding as above, one gets functionally the same results (4.1), (4.2) with a new renormalized DW temperature

$$\tilde{\tau} \equiv \tau I(\eta_\alpha, \eta, \tilde{\delta}) \tag{4.16}$$

where

$$I(\eta_\alpha, \eta, \tilde{\delta}) = \frac{c_0}{4P(\eta_\alpha)} \frac{\tilde{\delta}}{\sqrt{1 - \eta}} \ln \frac{\tilde{\delta}\sqrt{1 - \eta_\alpha} + \sqrt{1 - \eta}}{\tilde{\delta}\sqrt{1 - \eta_\alpha} - \sqrt{1 - \eta}}. \tag{4.17}$$

The latter simplifies in the limit $1 - \eta_\alpha \gg 1 - \eta$ to the second limiting expression in (4.7). It can be seen from (4.15) that in the case under consideration, $1 - \eta_\alpha \ll 1$, the integral (4.17) is determined by the long-wavelength region, which justifies using the continuous approximation for the transverse correlation function s. In the region of elliptic walls ($\tilde{\tau} < 1$) one has $\delta = \delta_B$ and hence in (4.17), $\tilde{\delta} = 1$. The critical values of both the DW-temperature τ and the absolute temperature θ (4.9) determined now by $I(\eta_\alpha, \eta, 1)$ go to zero in the uniaxial limit:

$$\tau_B \propto \theta_B \propto 1 \Big/ \ln \frac{1}{\eta - \eta_\alpha} \qquad \eta_\alpha \to \eta \tag{4.18}$$

which corresponds to the two-dimensional nature of the domain walls. One can see that the two-dimensional effects lead to a further decrease of the DW phase transition temperature: $\tau_B \equiv I^{-1}(\eta_\alpha, \eta, 1) < \tau_B^{(0)} \equiv I^{-1}(\eta_\alpha)$, where $I(\eta_\alpha)$ is given by (4.7).

In the linear-wall region ($\tilde{\tau} > 1$) the normalized wall width $\tilde{\delta}$ is given by the solution of the transcendental equation $\tilde{\delta}^2 = \tau I(\eta_\alpha, \eta, \tilde{\delta})$ following from (4.2) and (4.16). The latter can be rewritten in the natural units in the form

$$\delta_L = \frac{\sqrt{\alpha}}{2\epsilon} \frac{c_0}{P(\eta_\alpha)} \ln \frac{\delta_L + \xi_{c\alpha}}{\delta_L - \xi_{c\alpha}} \tag{4.19}$$

where $\xi_{c\alpha}$ is the transverse correlation length given by (3.19). Far from τ_B, where $\delta_L \gg \xi_{c\alpha}$, the solution of (4.19) leads to the formula (4.10). This asymptotic dependence can be also represented in the form $\tilde{\delta} = \sqrt{\tau I(\eta_\alpha)} = \sqrt{\tau/\tau_B^{(0)}}$, which is the analogue of the Curie–Weiss asymptote for the bulk susceptibility $\chi(T)$ of a ferromagnet far above T_c. In the purely isotropic model, $\eta_\alpha = \eta$, the linear DW structure is realized in the whole temperature range. The DW width δ_L determined by the solution of (4.19) shows a crossover to the Bloch-wall width δ_B at low temperatures:

$$\delta_L \cong \delta_B \left[1 + 2\exp\left(-\frac{2\epsilon}{\sqrt{1 - \eta}} \frac{P(\eta)}{c_0} \right) \right] \qquad \epsilon \equiv \theta_c/\theta - 1 \gg \sqrt{1 - \eta}. \tag{4.20}$$

It is worth noting that in this limiting case the longitudinal correlation length, $\xi_{cz} = \delta_L/2$, is determined by the transverse one, $\xi_{c\alpha} = \delta_B$.

The temperature dependencies of the DW order parameter $m_B \equiv \rho$ and the normalized DW width $\tilde{\delta}$ are represented in figure 2 for different values of η_α and $1 - \eta = 10^{-3}$. One can see that for $1 - \eta_\alpha = 10^{-2}$ the fluctuational decrease of the DW transition temperature is essential, although two-dimensional effects are still negligible in this case. In contrast,
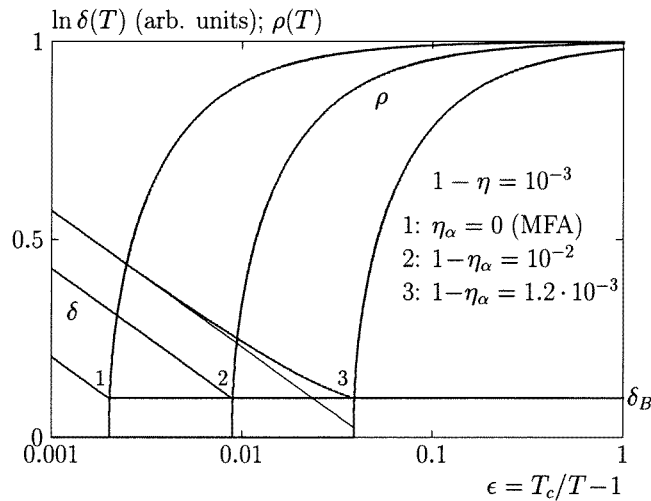
Figure 2. Temperature dependencies of the domain wall order parameter $m_B \equiv \rho$ and the DW width δ for different values of the second anisotropy parameter η_α.

for $1 - \eta_\alpha = 1.2 \times 10^{-3}$ they come into play, the corresponding additional diminishing of the transition temperature becomes essential, and the temperature dependence of $\tilde{\delta}$ in the logarithmic scale is no longer a straight line.

5. Discussion

In the main part of this paper the structure of domain walls in the biaxial ferromagnetic model described by the classical-vector Hamiltonian (2.1) was calculated exactly in the whole temperature range $T < T_c$ in the spherical limit $D \to \infty$. The main qualitative result is that in the purely uniaxial model ($\eta_\alpha = \eta$) the Bloch walls do not exist at any non-zero temperature (see equation (4.18)) being disordered by thermal fluctuations to the linear (Ising-like) ones. This result complements the well known fact that the Bloch walls in the purely uniaxial model (considered within the phenomenological micromagnetic approach which is equivalent to MFA) cannot move since their maximal velocity (the Walker velocity) is equal to zero. In the opposite limit, $\eta_\alpha = 0$, the model with $D \to \infty$ *total* spin components and a finite number (here two) of *interacting* ones is realized. In this case spin fluctuations die out and MFA becomes exact. The temperature of the phase transition from Bloch to linear walls T_B changes as a function of η_α from its MFA value $T_B = (1 - \epsilon_B)T_c$, $\epsilon_B = 2(1 - \eta) \ll 1$ at $\eta_\alpha = 0$ to 0 at $\eta_\alpha = \eta$ (see equations (4.3) and (4.9)).

In the actual case of a small anisotropy, $1 - \eta \ll 1$, the behaviour of a domain wall is more complicated than that of a purely two-dimensional object, since the DW width δ is much larger than the lattice spacing a_0. In the spherical limit this leads to the existence of two different mechanisms of the DW ordering, depending on the value of η_α. For the strong anisotropy in the basis plane 'x, y', $1 - \eta_\alpha \gg 1 - \eta$, the correlation length $\xi_{c\alpha}$ (3.19) for all temperatures is much shorter than the wall width δ (equation (4.2)), and the DW phase transition at T_B can be interpreted as the locally shifted bulk one (the 'perturbed three-dimensional' case, see equations (4.6)–(4.9)). In contrast, in the case of the two anisotropies comparable with each other, $1 - \eta_\alpha \sim 1 - \eta$, the true two-dimensional situation is realized (see equations (4.17) and (4.18)). Such a separation does not, however, persist

for models with finite values of D (e.g. for the Heisenberg model, $D = 3$), where the DW phase transition should always be of a two-dimensional character. For such models the fluctuations of the ordering spin components, m_z and m_y, also plays a role, and in the temperature interval about T_B, where the diverging correlation length ξ_{cy} exceeds the DW width δ, a two-dimensional behaviour is realized. Since $\delta \gg a_0$, this temperature interval should be much narrower than for a pure two-dimensional system. The asymptotic critical behaviour of the DW order parameter $m_B = \rho$ in (4.1) is described by the critical index $\beta_B = \frac{1}{8}$ of the two-dimensional Ising model, as was confirmed experimentally in [31, 32].

As a subject of future investigations, the temperature dependence of the DW magnetization profile in the self-consistent Gaussian approximation, without going to the limit $D \to \infty$, can be considered. Although it can be connected with more complicated numerical calculations, one can expect to obtain, with the help of SCGA, essentially more accurate results for domain walls in comparison with the spherical approximation, as was demonstrated for the bulk properties [40, 18]. The other problem is to formulate dynamic equations for fluctuating domain walls and to calculate their mobility. Such equations can, in principle, be obtained with the help of some dynamical generalization of the classical spin diagram technique [17]. Unfortunately, in the dynamical case one cannot make use of going to the limit $D \to \infty$ with all related simplifications, and only SCGA for the Heisenberg model can be used as the underlying static approach.

A promising field for the application of the methods of this paper is the surface effects in finite and semi-infinite magnetic systems, which are very sensitive to anisotropy. This problem was addressed recently in [12].

Acknowledgments

References

[1] Berlin T N and Kac M 1952 *Phys. Rev.* **86** 821
[2] Joyce G S 1972 *Phase Transitions and Critical Phenomena* vol 2, ed C Domb and M S Green (New York: Academic)
[3] Khorunzhy A M, Khoruzhenko B A, Pastur L A and Scherbina M V 1992 *Phase Transitions and Critical Phenomena* vol 15, ed C Domb and J L Lebowitz (New York: Academic)
[4] Barber M N and Fisher M E 1973 *Ann. Phys.* **77** 1
[5] Abraham D B and Robert M A 1980 *J. Phys. A: Math. Gen.* **13** 2229
[6] Singh S, Patria R K and Fisher M E 1986 *Phys. Rev.* B **33** 6415
[7] Allen S 1995 *J. Stat. Phys.* **79** 165
[8] Stanley H E 1968 *Phys. Rev.* **176** 718
[9] Stanley H E 1972 *Phase Transitions and Critical Phenomena* vol 3, ed C Domb and M S Green (New York: Academic)
[10] Knops H J F 1973 *J. Math. Phys.* **14** 1918
[11] Costache G, Mazilu D and Mihalache D 1976 *J. Phys. C: Solid State Phys.* **9** L501
[12] Garanin D A 1996 *J. Phys. A: Math. Gen.* submitted
[13] Abe R 1972 *Prog. Theor. Phys.* **48** 1414; 1973 *Prog. Theor. Phys.* **49** 113
[14] Abe R and Hikami S 1973 *Prog. Theor. Phys.* **49** 442; 1977 *Prog. Theor. Phys.* **57** 1197
[15] Okabe Y and Masutani M 1978 *Phys. Lett.* **65A** 97
[16] Okamoto H 1970 *Phys. Lett.* **32A** 315
[17] Garanin D A and Lutovinov V S 1984 *Solid State Commun.* **50** 219

D A Garanin

[18] Garanin D A *Phys. Rev.* B to be published
[19] Angelescu N, Bundaru M and Costache G 1981 *J. Phys. A: Math. Gen.* **14** L533
[20] Landau L D and Lifshitz E M 1935 *Z. Phys. Sov.* **8** 153
[21] Bulaevskii L N and Ginzburg V L 1964 *Sov. Phys.–JETP* **18** 530
[22] van den Broek J J and Zijstra H 1971 *IEEE Trans. Magn.* **MAG-7** 226
[23] Sarker S, Trullinger S E and Bishop A R 1976 *Phys. Lett.* **59A** 255
[24] Niez J J 1976 *J. Phys. C: Solid State Phys.* **9** 2933
[25] Lajzerowicz J and Niez J J 1979 *J. Physique* **40** L165
[26] Szymczak R, Maziewski A and Piotrowski K 1979 *J. Magn. Magn. Mater.* **12** 227
[27] Grahl M and Kötzler J 1989 *Z. Phys.* B **75** 527
[28] Kötzler J, Grahl M, Sessler I and Ferré J 1990 *Phys. Rev. Lett.* **64** 2446
[29] Panina L V, Garanin D A and Rusavin I G 1990 *IEEE Trans. Magn.* **MAG-26** 2816
[30] Garanin D A 1991 *Physica* **172A** 470; 1991 *Physica* **178A** 467
[31] Kötzler J, Garanin D A, Hartl M and Jahn L 1993 *Phys. Rev. Lett.* **71** 177
[32] Hartl-Malang M, Kötzler J and Garanin D A 1995 *Phys. Rev.* B **51** 8974
[33] Lawrie I D and Lowe M J 1981 *J. Phys. A: Math. Gen.* **14** 981
[34] Winter J M 1961 *Phys. Rev.* **124** 452
[35] Garanin D A 1994 *J. Stat. Phys.* **74** 275
[36] Vaks V G, Larkin A I and Pikin S A 1968 *Sov. Phys.–JETP* **26** 188
[37] Izyumov Yu A and Skryabin Yu N 1988 *Statistical Mechanics of Magnetically Ordered Materials* (New York: Consultants Bureau)
[38] Horwitz G and Callen H B 1961 *Phys. Rev.* **6** 1757
[39] Garanin D A and Lutovinov V S 1984 *Solid State Commun.* **49** 1049
[40] Garanin D A and Lutovinov V S 1986 *J. Physique* **47** 767